Traveltime-based anisotropic migration with angular parametrisation

T. Kaschwich, C. Vanelle, and D. Gajewski

email: *kaschwich@dkrz.de*

keywords: *migration, angular parametrisation, traveltimes, anisotropy*

ABSTRACT

Migration of seismic reflection data is a standard technique for subsurface imaging. To obtain a high quality image even illumination of the subsurface is essential. Conventional Kirchhoff migration, however, does not provide the desired angular coverage at the image point, especially when complex media are considered. In this paper we suggest a new strategy for migration with angular parametrisation in anisotropic media. The method, which guarantees even illumination, combines the conventional ray shooting with a hyperbolic traveltime interpolation. This makes the technique very efficient. An anisotropic example with elliptical symmetry confirms the high potential of the new strategy.

INTRODUCTION

Kirchhoff migration is one of the oldest migration tools, and has its roots in the graphical migration scheme of Hagedoorn (1954). His work was later related to the wave equation by Schneider (1978) and became familiar as "Kirchhoff migration". Kirchhoff migration is an inversion technique that images the structure of the subsurface from seismic reflection data. Even if newer migration methods exist that can in some cases provide better images, Kirchhoff migration is still a standard technique.

The conventional Kirchhoff migration treats each subsurface point under consideration as a diffraction point; the corresponding diffraction traveltime curves are constructed and the traces are stacked along that curve. In a typical seismic experiment, the source and the receivers are spaced uniformly in the recording surface. This line-up has, however, a vital disadvantage especially for complex subsurface structures: the usually equidistant spacing of source and receivers leads to high illumination in some angular regions, and poor illumination in others (see Figure 1). However for many purposes, e.g. AVO studies, an equiangular spacing at each image point is needed.

To overcome this deficiency, Brandsberg-Dahl et al. (2003) suggested a migration scheme with angular parametrisation. By following this strategy for migration, rays with equal angular spacing are required from the image point to the registration surface. Rays shot from image points with equiangular spacing, however, do not arrive at the recording surface with equidistant spacing (see Figure 1).

In this paper we introduce a migration method based on the idea of migration with angular parametrisation in combination with ray shooting and hyperbolic traveltime interpolation to calculate the traveltimes.

Therefore, we calculate traveltimes by ray shooting from each image point to the surface for each angle increment. Instead of applying seismic trace interpolation (Spitz, 1991), we calculate the traveltime to the real trace positions by applying the hyperbolic traveltime interpolation introduced by Vanelle and Gajewski (2002).

To account for the irregular grid resulting from the non-equidistant positions in the registration surface, we extended the hyperbolic traveltime interpolation. During the migration procedure only those traces, which are accessible from the image point, are taken into account. To obtain an image with high-resolution, the subsurface is discretised on a fine grid. Since traveltimes to the registration surface are required for each

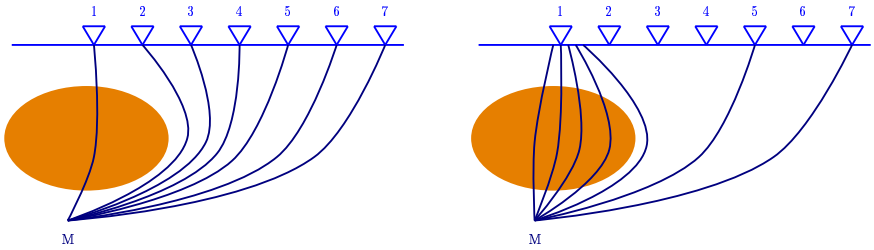

Figure 1: Both figures demonstrate a model with a negative velocity lens structure. The left hand side figure shows the principle of the conventional Kirchhoff migration, where the registration surface has an equidistant sampling, but this is no guarantee that this is also the case at the image point; the right figure shows the situation for the migration with angular parametrisation, where even illumination at the image point is ensured.

image point on that fine migration grid, we also use hyperbolic interpolation of the traveltimes at the image point. Then, ray shooting has only got to be carried out for image points on a coarse grid.
After an introduction to the method we give a numerical example. We demonstrate the accuracy of the technique by comparing traveltimes computed for an anisotropic model to exact traveltimes. Additionally, we show the migration results for the presented model. Finally, we will conclude our results and present an outlook to future work.

THE METHOD

In this part, we give a short overview of our traveltime-based migration implementation with angular parametrisation. Also, we explain the extension of the hyperbolic traveltime expansion (Vanelle and Gajewski, 2002) for our application.
Inside a predefined target zone (see Figure 2(a)) traveltimes are calculated from image points on a coarse grid to the registration surface. To provide the desired uniform angular coverage at the image point M the slowness at M is defined by equidistant emergence angles (see Figure 2(b)). To calculate the traveltimes by ray shooting from the image point M to a point at the surface we solve the kinematic ray tracing system (Červený, 1972). Since in most cases there will be no source or receiver at this position, the hyperbolic traveltime interpolation is applied. For this purpose we have extended the hyperbolic traveltime approach by Vanelle and Gajewski (2002) to irregular traveltime grids. This approach allows us to interpolate the traveltimes to the real trace position (Figure 2(c)). We use the same method to interpolate to image points on a fine grid (Figure 2(d)).

Hyperbolic traveltime equation for irregular grids

To interpolate the traveltimes from the intersection points of the rays with the registration surface to the receiver position we use the 3-D hyperbolic traveltime expansion introduced by Vanelle and Gajewski (2002). It follows from a Taylor expansion of the squared traveltime T^2. The expansion is carried out in the three components of the source position vector $\vec{s} = (s_1, s_2, s_3)$ and those of the receiver positions $\vec{g} = (g_1, g_2, g_3)$. The hyperbolic equation reads

$$T^2(\vec{s},\vec{g}) = (T_0 - \vec{p}_0^{\,T}\Delta\vec{s} + \vec{q}_0^{\,T}\Delta\vec{g})^2 + T_0\left(-2\Delta\vec{s}^{\,T}\underline{\mathsf{N}}\Delta\vec{g} - \Delta\vec{s}^{\,T}\underline{\mathsf{S}}\Delta\vec{s} + \Delta\vec{g}^{\,T}\underline{\mathsf{G}}\Delta\vec{g}\right) + \mathcal{O}(3), \quad (1)$$

where T_0 is the traveltime in the expansion point. The "source" location here is assumed to be the image point, and the receiver in the registration surface. Therefore, here the expansion point corresponds to the "source" on the coarse subsurface grid and the receiver at the endpoint of the ray in the registration surface. The vectors $\Delta\vec{g} = \vec{g} - \vec{g}_0$ and $\Delta\vec{s} = \vec{s} - \vec{s}_0$ are the deviations of the image point and receiver positions ($\vec{s}$ and $\vec{g}$) from the location of the expansion point ($\vec{s}_0$ and $\vec{g}_0$).

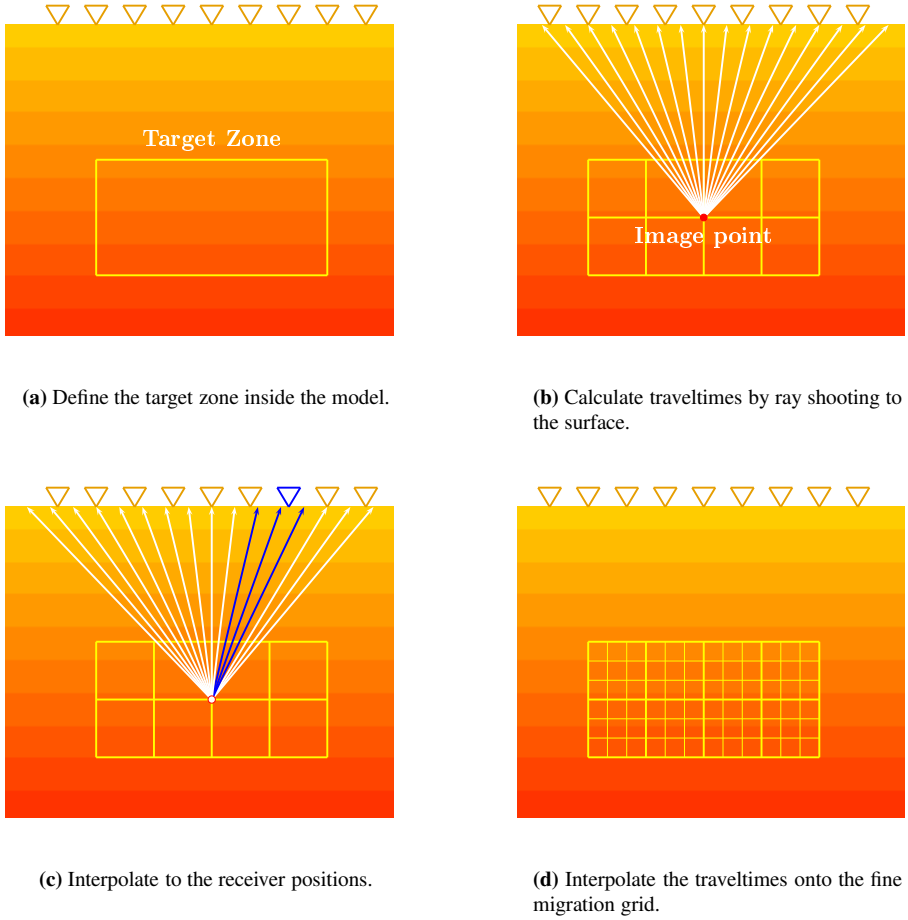

(a) Define the target zone inside the model.

(b) Calculate traveltimes by ray shooting to the surface.

(c) Interpolate to the receiver positions.

(d) Interpolate the traveltimes onto the fine migration grid.

Figure 2: The principle of calculating the traveltime tables for the migration procedure.

The first-order derivatives

$$p_{i_0} = -\left.\frac{\partial T}{\partial s_i}\right|_{\vec{s}_0\vec{g}_0} \quad \text{and} \quad q_{i_0} = -\left.\frac{\partial T}{\partial g_i}\right|_{\vec{s}_0\vec{g}_0}, \tag{2}$$

are the slowness vectors at the image point and the receiver, and the matrices

$$\begin{aligned} S_{ij} &= -\left.\frac{\partial^2 T}{\partial s_i \partial s_j}\right|_{\vec{s}_0\vec{g}_0} = S_{ji}, \\ G_{ij} &= \left.\frac{\partial^2 T}{\partial g_i \partial g_j}\right|_{\vec{s}_0\vec{g}_0} = G_{ji}, \\ N_{ij} &= -\left.\frac{\partial^2 T}{\partial s_i \partial g_j}\right|_{\vec{s}_0\vec{g}_0} \neq N_{ji}, \end{aligned} \tag{3}$$

$(i, j = 1, 2, 3)$ are the second derivatives of the traveltimes, which are related to the curvature of the wavefront.

We will now consider one expansion point. The receiver position of the expansion point is defined by the emergence angle at the image point. The coefficients G_{xx} and q_{x0} can be computed from the three traveltime values $T_0 = T(\vec{s}_0, \vec{g}_0)$, $T_m = T(\vec{s}_0, \vec{g}_0 - \Delta g_m)$ and $T_p = T(\vec{s}_0, \vec{g}_0 + \Delta g_p)$ (see Figure 3(a)). In

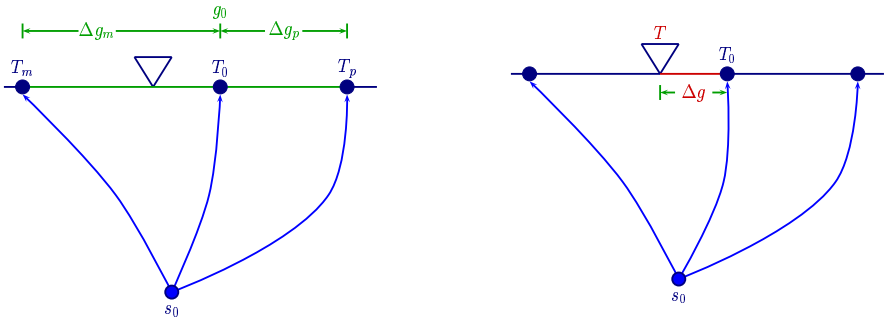

(a) First step: Determination of the traveltime coefficients q_x and G_{xx} at position g_0.

(b) Second step: Interpolation to the real receiver position g.

Figure 3: Traveltime interpolation to the real receiver position. The traveltimes T_m, T_0 and T_p are computed by ray shooting.

comparison to the regular grid formula given by Vanelle and Gajewski (2002), here the distances between grid points differ ($\Delta g_m \neq \Delta g_p$). The insertion of T_m and T_p into the hyperbolic equation (1) leads to a linear system of two equations with two unknowns, which can be solved for q_{x0} and G_{xx}. As result we get

$$\begin{aligned} q_{x0} &= \frac{T_p^2\Delta g_m^2 - T_m^2\Delta g_p^2 - T_0^2(\Delta g_m^2 + \Delta g_p^2)}{2T_0(\Delta g_m^2\Delta g_p + \Delta g_m\Delta g_p^2)}, \\ G_{xx} &= \frac{T_m^2\Delta g_p + T_p^2\Delta g_m - T_0^2(\Delta g_m + \Delta g_p)}{T_0(\Delta g_m^2\Delta g_p + \Delta g_m\Delta g_p^2)} + \frac{q_{x0}^2}{T_0}. \end{aligned} \tag{4}$$

After the coefficients have been determined, Equation (1) can be directly applied for the traveltime interpolation to the real receiver position g (see Figure 3(b)). This is repeated for all receiver positions and for each subsurface point.

Interpolation to the fine migration grid

It is also possible to interpolate traveltimes between image points, i.e. $\Delta\vec{s} \neq 0$. This requires that the derivatives with respect to the image point positions are also known. The coefficients S_{xx}, p_{x0} can be obtained from the traveltimes T_m and T_p (see Figure 4).
The ray shooting from the three subsurface points s_m, s_0 and s_p gives us the traveltimes T_m^0, T_0 and T_p^0. By applying the hyperbolic traveltime interpolation with the coefficients q_m and G_m for the expansion point (s_m, g_m) which we have already calculated before, we get (see also Figure 4)

$$T_m^2 = (T_m^0 - q_m\Delta g_m)^2 - T_m^0 G_m \Delta g_m^2. \tag{5}$$

Similar, interpolation with the coefficients q_p and G_p at (s_p, g_p) yields

$$T_p^2 = (T_p^0 - q_p\Delta g_p)^2 - T_p^0 G_p \Delta g_p^2. \tag{6}$$

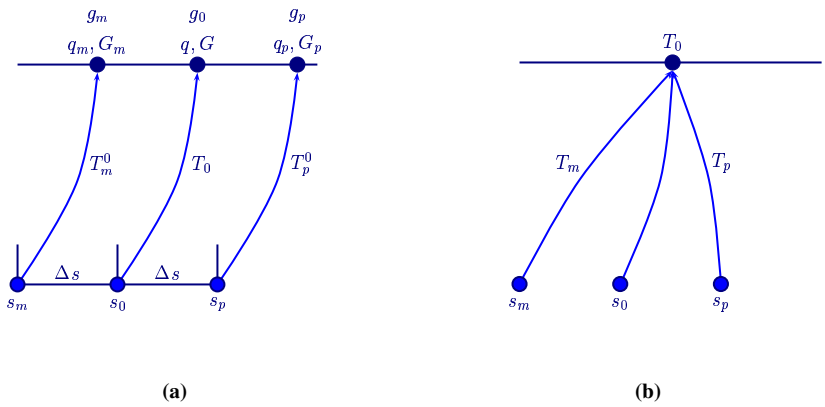

Figure 4: (a) Rays are shot from the three subsurface points at s_m, s_0 and s_p, respectively. The corresponding traveltimes to the surface are T_m^0, T_0 and T_p^0.(b) With the coefficients q_m, q_p, G_m and G_p we obtain the traveltimes T_m and T_p. These lead to the coefficients p_{x0} and S_{xx}.

With these traveltimes we can calculate the coefficients p_{x0} and S_{xx}:

$$\begin{aligned} p_{x0} &= \frac{T_m^2 - T_p^2}{4T_0\Delta s}, \\ S_{xx} &= \frac{T_p^2 + T_m^2 - 2T_0^2}{2T_0\Delta s^2} - \frac{p_{x0}^2}{T_0}, \end{aligned} \tag{7}$$

where $\Delta s = s_p - s_0 = s_0 - s_m$. The remaining coefficients are computed correspondingly. Afterwards the traveltimes can be interpolated from the fine grid of image points to the receiver positions.

NUMERICAL EXAMPLE

Traveltime interpolation

To illustrate the accuracy of the traveltime computation presented in the previous section we have chosen an anisotropic two-layers model with elliptical symmetry. Elliptical anisotropy is a special case of polar anisotropy with an additional constraint, that reduces the number of independent elastic parameters to four. Elliptical anisotropy is rarely found in real rocks. It is used here for verification purposes since traveltimes and synthetic seismograms can be computed analytically. We describe our model by the Thomson parameters $\epsilon = \delta = 0.187$ and $\gamma = 0.51$ and the vertical velocities v_{p0} and v_{s0} (Thomsen, 1986). The model is shown in Figure 5. The receivers are located at the surface with 20 m spacing.

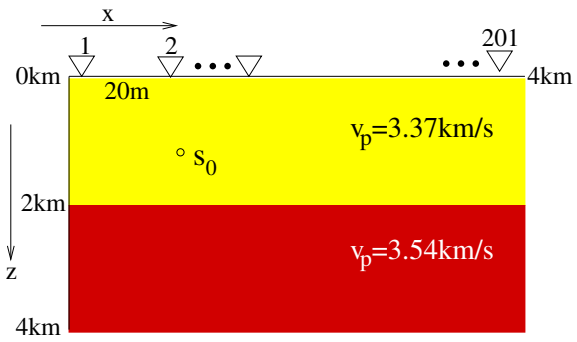

Figure 5: The model dimensions for the elliptically anisotropic test model.

To evaluate the accuracy of the traveltime interpolation, we will consider an image point at $s_0 = (0.5, 0.5)$km. From here and the neighbouring image points on a 100 m coarse grid we have performed ray shooting with a constant angular increment. Traveltimes were interpolated from four different image points to the receivers using (1) and were compared to analytic values. The results are shown in Figure 6.

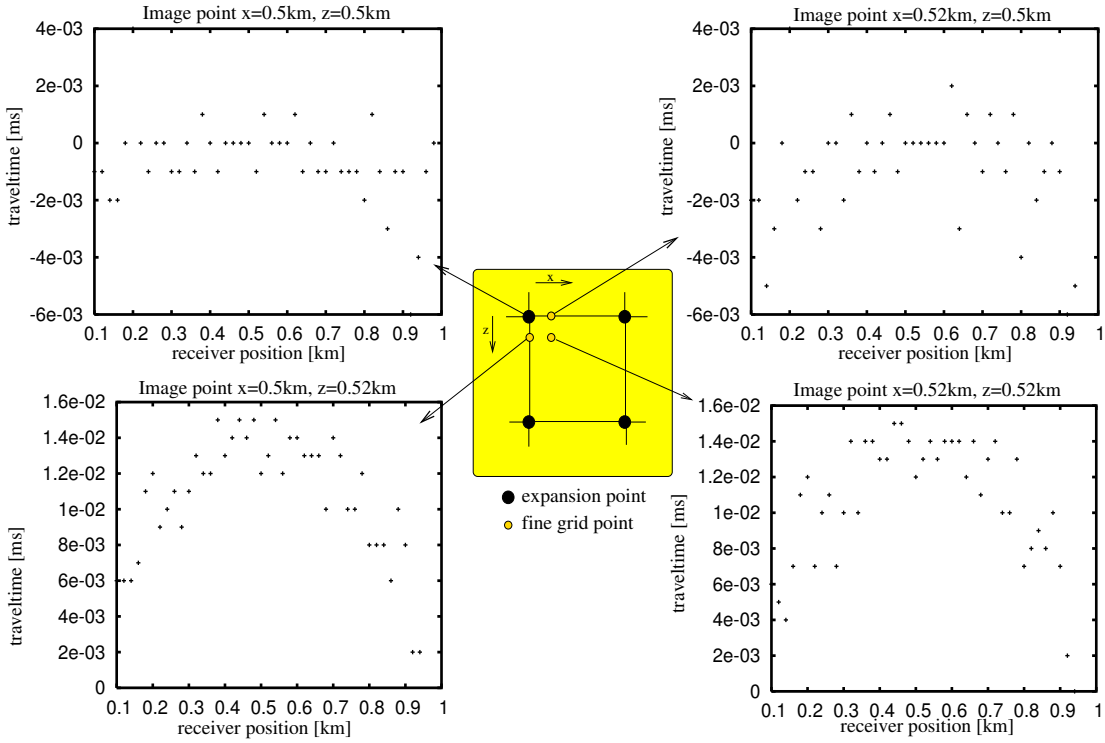

Figure 6: Distribution of traveltime errors. Upper left: errors for an image point on the coarse grid at $\vec{s}_0 = (0.5, 0.5)$km. Upper right: errors for an image point of the fine grid with $\vec{s} = (0.52, 0.5)\ \Delta x = 20m$. Lower left: errors for an image point at $\vec{s} = (0.5, 0.52)\ \Delta z = 20m$. Lower right: Errors distribution for an image point of the fine grid with $\vec{s} = (0.52, 0.52)\ \Delta x = \Delta z = 20m$.

The upper figure on the left hand side shows the absolute traveltime error for the image point on the coarse grid, i.e.at $\vec{s}_0 = (0.5, 0.5)$km. Here, we have the lowest errors, because we only had to interpolate the receiver positions. The absolute traveltime error is less than 0.004 ms for all receiver positions.
The upper figure on the right hand side and the lower figure on the left side represent the absolute errors for image points on the fine grid, where we have interpolated traveltimes for image points at the positions $\vec{s} = (0.52, 0.5)\ \Delta x = 20m$ and $\vec{s} = (0.5, 0.52)\ \Delta z = 20m$. While we have slightly better results for the fine grid interpolation in x-direction, the maximum absolute traveltime error in z-direction is also less than 0.016 ms.
The lower figure on the right side shows the error distribution for an image point at the position $\vec{s} = (0.52, 0.52)\ \Delta x = \Delta z = 20m$. In this case the absolute traveltime error is also lower than 0.016 ms.
The interpolation of traveltimes onto the fine grid was 10 times faster than the calculation with ray shooting from image points on the fine grid.
We have chosen a homogeneous medium with elliptical symmetry to validate our implementation. For this medium, the traveltime expression (1) is exact. Therefore, we expected traveltime errors within machine precision, which was confirmed by the tests. The high accuracy of the traveltime interpolation for other types of complex isotropic and anisotropic media for regular grids was already demonstrated in Vanelle and Gajewski (2002) and Vanelle and Gajewski (2003).

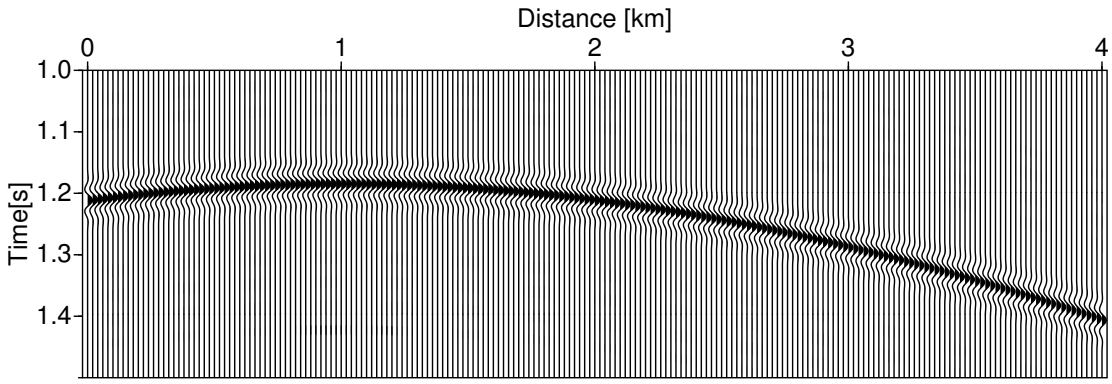

Figure 7: Synthetic common-shot section: The receiver spacing is 20 m and the source is located at 1 km.

Migration

To verify the migration algorithm synthetic seismograms in a common-shot configuration were computed for the two-layers model. The seismograms were computed using the analytical solution. The synthetic shot section (Figure 7) was created with a receiver spacing of 20 m, where the source is located at 1 km. The input traveltimes were calculated on a 100 m grid. First the interpolation to a fine migration grid is accomplished, here the grid spacing is 5 m. These traveltimes were the only input data for the migration algorithm.
Figure 8 shows the migrated depth section. The reflector has been migrated to the correct depth. The hyperbola-shaped event in the migrated section is an artefact caused by the limited extent of the receiver line. It can be suppressed by application of a suitable taper.

CONCLUSION AND OUTLOOK

We have presented a traveltime-based implementation for the migration with angular parametrisation. The traveltimes are computed on coarse grids, leading to considerable savings in storage. Subsequent hyperbolic interpolation leads to the traveltimes on the required fine migration grid. A numerical example indicates the quality of the traveltime interpolation. Application of angle-based migration to a simple anisotropic model resulted in a kinematically correct image of the subsurface where the reflector depth was successfully reconstructed.
The main advantage of the migration with angular parametrisation in comparison to conventional migration is that it leads to an even illumination. This is especially important for media with a complex subsurface structure. Therefore, future work will be devoted to compare the migration results of traveltime-based migration with angular parametrisation with conventional Kirchhoff migration for heterogeneous complex 3-D models.
The consideration of migration amplitudes is another important future aspect. The output of a true-amplitude migration serves as input for AVO analysis, a key technique for reservoir characterisation. Future work will therefore be addressed to the extension of the angle-based implementation to true-amplitude migration in anisotropic media. This implementation will also be based on traveltimes as only input information for the determination of the true-amplitude weights.

ACKNOWLEDGEMENTS

This work was kindly supported by the German Research Society (grants Ga 350/10-2 and Va 207/3) and the sponsors of the *Wave Inversion Technology (WIT) Consortium*. Continuous discussions with the members of the Applied Geophysics Group Hamburg are appreciated.

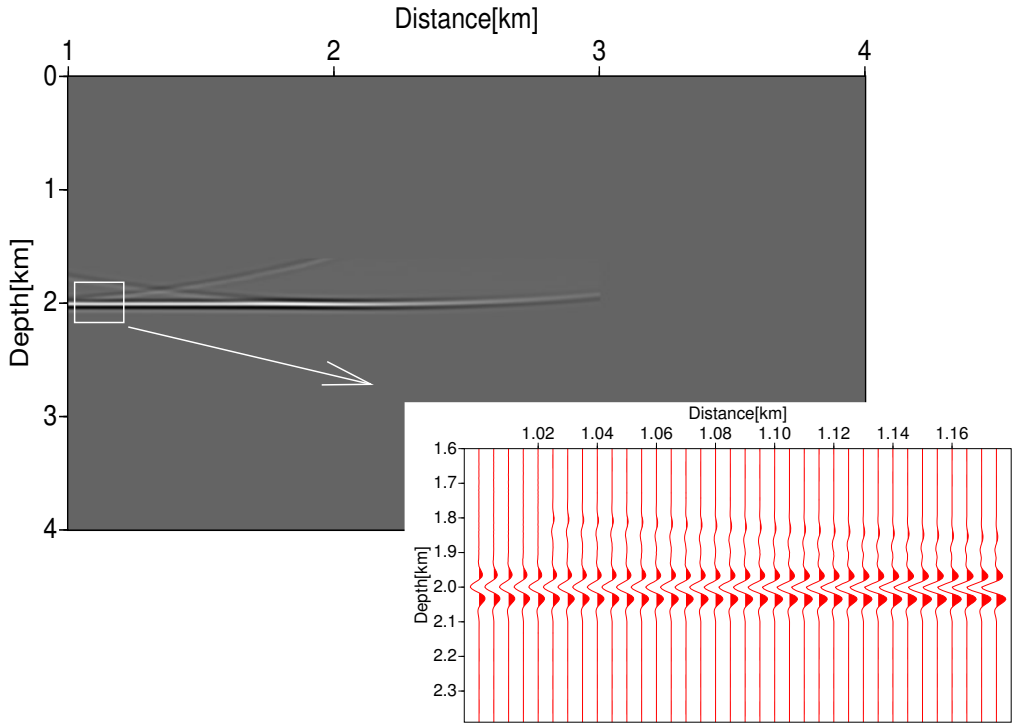

Figure 8: Migrated depth section of the common shot section shown in Figure 7. The reflector was migrated to the correct depth. The hyperbola-shaped artefact is an aperture effect which can be removed by applying a taper.

REFERENCES

Brandsberg-Dahl, S., de Hoop, M., and Ursin, B. (2003). Focusing in dip and AVA compensation on scattering-angle/azimuth common image gathers. *Geophysics*, 68:232–254.

Červený, V. (1972). Seismic Rays and Ray Intensities in Inhomogeneous Anisotropic Media. *The Geophysical Journal of the Royal Astronomical Society*, 29:1–13.

Hagedoorn, J. (1954). A process of seismic reflection interpretation. *Geophysical Prospecting*, 2:85–127.

Schneider, A. (1978). Integral formulation for migration in two and three dimension. *Geophysics*, 43:49–76.

Spitz, S. (1991). Seismic trace interpolation in the f-x domain. *Geophysics*, 56:785–794.

Thomsen, L. (1986). Weak elastic anisotropy. *Geophysics*, 51:1954–1966.

Vanelle, C. and Gajewski, D. (2002). Second-order interpolation of traveltimes. *Geophysical Prospecting*, 50:73–83.

Vanelle, C. and Gajewski, D. (2003). Determination of geometrical spreading from traveltimes. *Journal of Applied Geophysics*, 54:391–400.